

THERMOGRAVIMETRY OF CHITOSAN WITH NANOFILLERS

Anna Puchalska, Maria Mucha

*Technical University of Lodz,
Faculty of Process and Environmental Engineering,
ul. Wolczanska 213, 90-924 Łódź, Poland
E-mail: puchalsk@wipos.p.lodz.pl*

Abstract

In the present paper the degradation of chitosan and its blends with hydroxyapatite, nanoclay and nanosilver as well as the impact of those nanofillers added to chitosan on its decomposition at high temperatures are studied. The applied films of thickness 50 μm were obtained by casting the acidic solutions: chitosan and its blends with hydroxyapatite, nanoclay and nanosilver. To mix solutions with nanofillers ultrasounds were applied. To study the thermal degradation we applied thermogravimetry in dynamic and static conditions, which is a method of thermal analysis involving the continuous recording of weight loss. Based on experimental data activation energies of thermal decomposition close to a maximum rate loss were calculated using different methods for chitosan and its blends with hydroxyapatite, nanoclay and nanosilver. The addition of three nanofillers mentioned above result in a visual increase of activation energy of thermal degradation process of chitosan due to slower evolution of decomposed gases from chitosan matrix reflected by a slower rate of weight loss.

Key words: *biopolymers, chitosan, thermogravimetry, activation energy.*

1. Introduction

The non-biodegradable polymers in the vast majority being produced from fossil fuels have contributed to a substantial disturbance and damage of the natural ecosystem. Therefore, scientists respond to this need developing renewable source-based biopolymer materials whose production process would not involve the use of toxic and harmful components. Ideally, biopolymer materials should degrade via a natural composting process. Seemingly, polysaccharides such as chitosan are most promising as they originate from naturally abundant products and are readily biodegradable [1].

Chitosan is a linear copolymer composed of β (1-4)-linked 2-acetamido-2-deoxy- β -D-glucopyranose and β (1-4) 2-amino-2-deoxy-D-glucopyranose units [2]. It occurs as a component of the cell wall of some fungi but it is generally produced by carrying out the deacetylation of chitin, an abundant polysaccharide found in the shells of crustaceans, particularly crabs and shrimps. Due to its special physical, chemical and biological properties chitosan has extensive applications in the food industry, agriculture, pharmacy and medicine and waste water treatment. Indeed, chitosan is a biocompatible and biodegradable polymer whose degradation pathway has been studied by various methods [3, 4]. It should be highlighted that chitosan, analogously to other biopolymers, displays a high sensitivity to various types of degradation, e.g. oxidative, hydrolytic, thermo-, photo- and ultrasonic degradation. What is more, to apply pure chitosan, in blends and its composites with other polymers it is required that it should be exposed to heat, light, water and microorganisms with a possible degradation of the macromolecular chain. Based on previous results of weight loss and FTIR spectra investigations it was found that there was a definite effect of the deacetylation degree of chitosan on the rate of a degradation process that took place under the influence of ultraviolet light or at high temperatures up to 200 °C. In the case of photodegradation, the chitosan of the highest DD value is degraded the fastest rate which is due to the largest contribution of chromophore amine groups that absorb UV radiation. The results of spectroscopic studies show that both photodegradation and thermal degradation lead first of all scission of the main chain and destruction of the unstable amine groups. It was observed that chitosan DD decreases in the process of thermodestruction; cross-linking of chitosan macromolecules takes place which enhances thermal stability of the polymer in the next stage. At the temperature range up to 230 °C the thermodegradation rate is higher for chitosan samples of large DD (higher weight loss in dynamic and isothermal measurements). At the temperature range at a maximum rate of weight loss, the chitosan sample of higher DD is more stable (also the activation energy of the reaction is higher). Thermodegradation of chitosan in the air atmosphere causes oxidation of the sample (absorbance of carbonyl increases the band).

Certain properties of chitosan such as: thermal stability, hardness, barrier to gases may prove to be insufficient for application in several fields, therefore, one of the methods more and more frequently applied to enhance those properties is adding such nanofillers as hydroxyapatite, nanoclays and nanosilver. In recent years, hydroxyapatite (HA) nanoparticles have been widely used as reinforcing fillers in biomedical materials. Nanoclays (montmorillonite) have been used as reinforcing filler to improve mechanical and barrier properties of polymers. Silver exhibits good anti-bacterial properties and in recent years has

been used on medical devices ranging from wound dressings to urinary catheters. In addition to silver's anti-bacterial properties it also seems to possess anti-inflammatory properties and improved healing rates. The anti-bacterial activity of silver is dependent on the silver cation (Ag^+), which binds strongly to electron donor groups on biological molecules containing sulfur, oxygen or nitrogen [5].

2. Theoretical background of thermogravimetry

The thermogravimetric analysis has been widely used by many authors to investigate the stability of polymers. Nevertheless, although the mathematical description of the decomposition process of polymers in the solid state relies on three kinetic components, namely the two Arrhenius parameters, activation energy (E_a) and pre-exponential factor (A) and the analytical expression describing the kinetic model $f(\alpha)$, the former parameter (E_a) is the most frequently used to discuss the thermal stability. Isothermal and dynamic conditions and many different methods have been employed to determine E_a of chitosan and its composites in argon atmosphere.

At the onset of the kinetic analysis of a thermal degradation process one may express the reaction rate by a general equation such that [6]:

$$\frac{d\alpha}{dt} = k(T)f(\alpha) \quad (1)$$

where t denotes the time, α – is the conversion degree, T is the temperature, $k(T)$ is the temperature-dependent rate constant and $f(\alpha)$ is a temperature-independent function that represents the reaction model. The rate constant $k(T)$ is given, generally, by the Arrhenius equation:

$$k(T) = A \exp\left(-\frac{E_a}{RT}\right) \quad (2)$$

Where A is the pre-exponential or frequency factor and E_a is the apparent activation energy. Thus, **Equation 1** may be rewritten as:

$$\frac{d\alpha}{dt} = A \exp\left(-\frac{E_a}{RT}\right) f(\alpha) \quad (3)$$

or if $\beta = \frac{dT}{dt}$ - the heating rate

$$\frac{d\alpha}{dT} = \frac{1}{\beta} \frac{d\alpha}{dt} = \frac{A}{\beta} \exp(-E_a/RT) (1-\alpha)^n \quad (4)$$

Separation of variables leads to the following expression:

$$\frac{d\alpha}{(1-\alpha)^n} = \frac{A}{\beta} \exp\left(-\frac{E_a}{RT}\right) dT \quad (5)$$

Equations 4 and **5** may serve as a basis for calculation of kinetic parameters (E_a , A and n) of a thermal process of polymer decomposition. Calculations may be performed as follows:

- using the above equations directly (one may find a logarithm of these equations and then find a differential and substitute the data in a differential form);
- integrating those differential equations.

To find a kinetic activation energy the following methods have been applied:

- a. Method by Freeman – Carroll [7] is one of the frequently applied methods according to which, taking into consideration logarithmic changes of the values $d\alpha/dT$, $(1-\alpha)$ determined from the kinetic curves (**Figure 2**) the following equation is obtained:

$$\frac{\Delta \ln\left(\frac{d\alpha}{dT}\right)}{\Delta \ln(1-\alpha)} = \frac{E_a \Delta\left(\frac{1}{T}\right)}{R \Delta \ln(1-\alpha)} + n \quad (6)$$

One may obtain E_a and n respectively from the slope plotting the left side of the **Equation 7** versus $\frac{\Delta\left(\frac{1}{T}\right)}{\Delta \ln(1-\alpha)}$.

- b. In the method proposed by Ozawa [8] the function $F(\alpha)$ in the following equation:

$$\log F(\alpha) = \log\left(\frac{AE_a}{R}\right) - \log \beta - 2.315 - \frac{0.4567E_a}{RT} \quad (7)$$

for $n = 1$, $F(\alpha) = h \frac{1}{1-\alpha}$

Plotting $\log \beta$ versus $1/T$ one may obtain straight lines for a given conversion degree which may serve for calculation of activation energy E_a .

- c. Activation energy for decomposition E_a of the polymer blends and nanocomposites can be calculated from the TGA curves by the integral method proposed by Horowitz and Metzger [9] using the equation as follows:

$$\ln[\ln(1-\alpha)]^{-1} = \frac{E_a \theta}{RT_{\max}^2} \quad (8)$$

where α is the conversion degree (decomposed fraction), E_a – is the activation energy of decomposition, T_{\max} – is the temperature at maximum rate of weight loss, θ is $(T - T_{\max})$, and R is the gas constant.

From the plots of $\ln[\ln(1-\alpha)^{-1}]$ versus θ , the activation energy (E_a) for decomposition can be determined from the slope of the straight line of the plots.

- d. Isothermal method [10]

The kinetic equation of isothermal processes may be written in the following form:

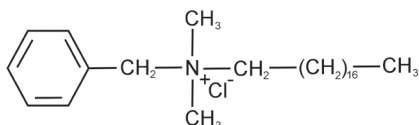
$$\ln \frac{d\alpha}{dt} = \ln A + n \ln(1-\alpha) - \frac{E_a}{RT} \quad (9)$$

Plotting the dependence $\ln d\alpha/dt$ in the function $\ln(1-\alpha)$ one may also obtain a reaction order n from the slope. Then the values of ordinate for $\ln(1-\alpha)=0$ plotted in the function $1/T$ allow one to calculate pre-exponential parameter and activation energy of the initial stage of degradation.

3. Materials and methods

3.1. Materials used

Chitosan (CH) (poly-2-aminoglucose) of deacetylation degree DD=85% and molecular weight $M = 2.1 \times 10^5$, was produced by Biotechnologie und Logistik GmbH. It is a biodegradable natural copolymer obtained by chitin modification. Hydroxyapatite (H) was produced by Sigma Aldrich. It belongs to the family of minerals known as apatites and its structure is $\text{Ca}_{10}(\text{PO}_4)_6(\text{OH})_2$. Hydroxyapatite has the ratio of calcium to phosphorus equal to 1.67. Nanoclay (N) - Nanofil 2 produced by Süd Chemie is montmorillonite modified by ammonium salt. The structure of an organophilization agent (sterylbenzyl dimethyl ammonium chloride) for Nanofil 2 (N2) is as follows:



3.2. Preparation of composites

After chitosan (CH) of deacetylation degree DD = 85% was dissolved in pH 4 acetic acid, organoclay nanofil 2 (N) or hydroxyapatite (H) were added in the % weight fraction 2 and 10% and the mixture was stirred at ambient temperature using ultrasounds. Nanosilver (Ag) was obtained on the way of mixing the solutions of ascorbic acid (0.1 M), chitosan and silver nitrate (0.1 M) (in which its reduction takes place) for three hours at ambient temperature. Nanocomposite films about 50 μm thick were prepared by casting and solvent evaporation. Exfoliation of Nanofil 2 in chitosan was noted by the Authors previously [11].

3.3. Microscopic analysis of morphological structure

There was carried out - morphological analysis using optical microscope MINTRON OS55D. Optical electron microscopy examination shows good dispersion of nanoclay, hydroxyapatite and nanosilver fillers in biopolymer matrices which is desirable for a uniform composite.

As regards the dispersion of the nanofillers in the film, one may distinguish here a structure where silicate, hydroxyapatite and nanosilver are completely homogeneously dispersed in the polymer matrix. Due to the hydrophilic and polycationic nature of chitosan in acidic media, this biopolymer has good miscibility with nanofil by means of cationic exchange. The nanofillers dispersion within chitosan has been characterized by optical microscopy (**Figures 1** and **2**). As regards microscopic observation, we do not include the photograph of chitosan with hydroxyapatite as in the case of hydroxyapatite an atomic dispersion occurs which is not to be observed under the optical microscope.

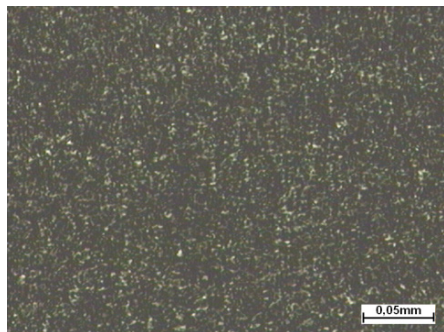


Figure 1. Chitosan with Nanofil (10%).

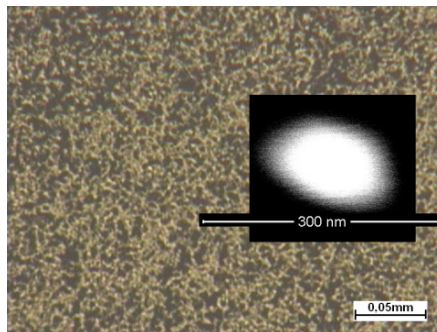


Figure 2. Chitosan with nanosilver (10%).

3.4. Measuring methods

Prepared films were subjected to thermal analysis using a thermo-analyzer (NETZSCH STA 409PG Luxx) in argon atmosphere. Thermogravimetry was carried out in dynamic conditions: heating rates : 5, 10, 15 K/min from the ambient temperature to 450 °C and in isothermal conditions at temperatures 220, 230 and 240 °C.

4. Results and discussion

In the following **Figures 3 - 8** the thermogravimetric measurements and results of calculations are presented.

4.1. Dynamic experiments

Figures 3 - 4 show TG and DTG curves obtained for chitosan with hydroxyapatite, nanofil 2 and nanosilver composites. One should also consider **Figure 3** showing TG curves of chitosan and chitosan nanocomposites (chitosan with hydroxyapatite, nanoclay

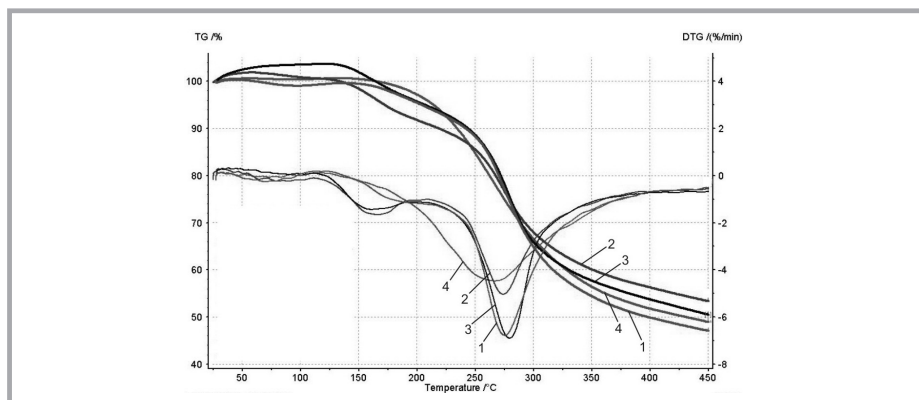


Figure 3. TG and DTG curves of pure chitosan and chitosan composites. Weight fraction of nanofillers equal to 10% by weight. 1 denotes chitosan (CH), 2– chitosan with hydroxyapatite (CHH), 3 – chitosan with nanofil (CHN), 4 – chitosan with nanosilver (CHAG).

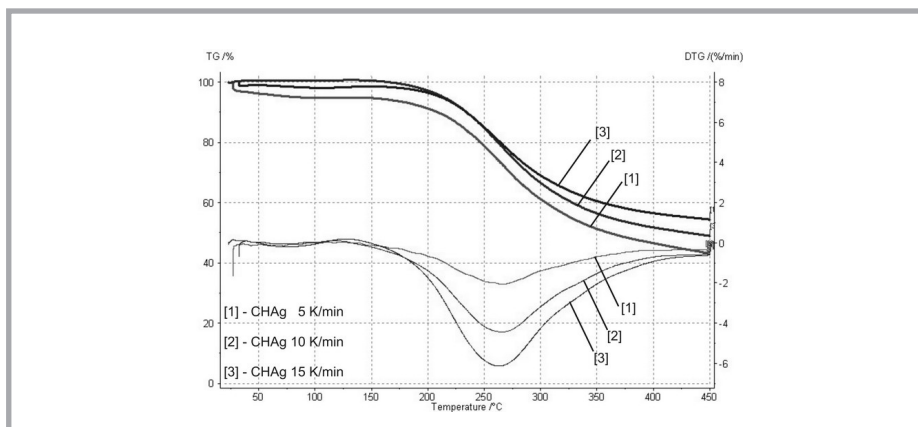


Figure 4.a. TG and DTG curves of chitosan with nanosilver (10%) at different heating rates. 1 – denotes CHAg at 5 K/min; 2 – CHAg at 10 K/min; 3 – CHAg at 15 K/min.

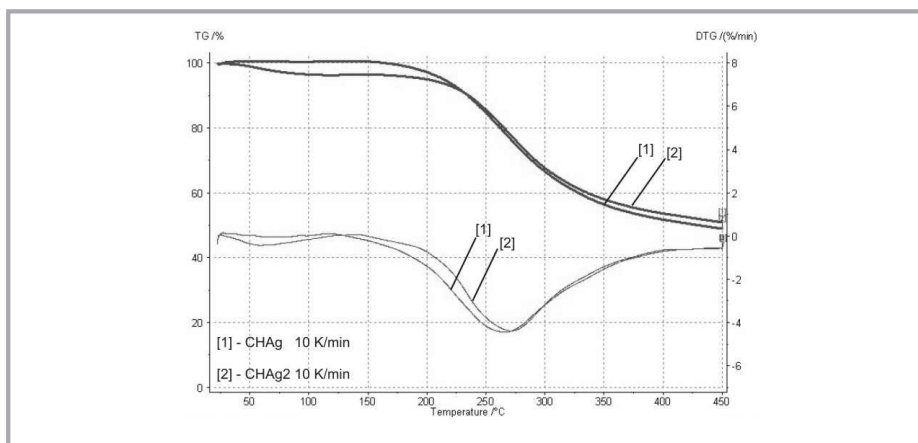


Figure 4.b. TG and DTG curves of [1] chitosan with nanosilver 10% and [2] – chitosan with nanosilver 2% at the heating rate 10 K/min.

and nanosilver) at heating rate 10 °C/min. At this stage, the thermogravimetric analysis was performed for the weight loss due to volatilization of the degradation products was monitored as a function of temperature. It can be presumed that the observed small improvement of thermal stability of the composites is attributed to the shielding effect of the clay, hydroxyapatite and nanosilver that means that degradation products can have a long way around the nonorganic compounds additives to leave the sample [12, 13]. The TG and DTG curves of chitosan with silver of two various weight fractions (2 and 10%) at different heating rates (β) from room temperature to 450 °C in argon atmosphere are shown in **Figure 4**. The TG curves show a first thermal step in the range 25 – 140 °C corresponding to a weight loss of approximately 6% and it is attributed to the evaporation of water loosely bound to

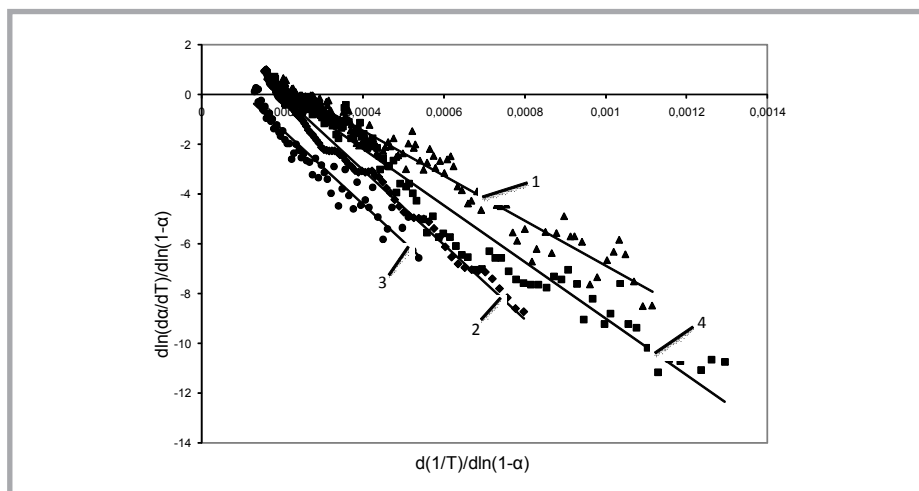


Figure 5. Plot of $d\ln(d\alpha/dT)/d\ln(1-\alpha)$ versus $d(1/T)/d\ln(1-\alpha)$ (Equation (6)). Weight fraction of a nanofiller equal to 10%. 1 – CH; 2]– CHH; 3 – CHN; 4 – CHAg.

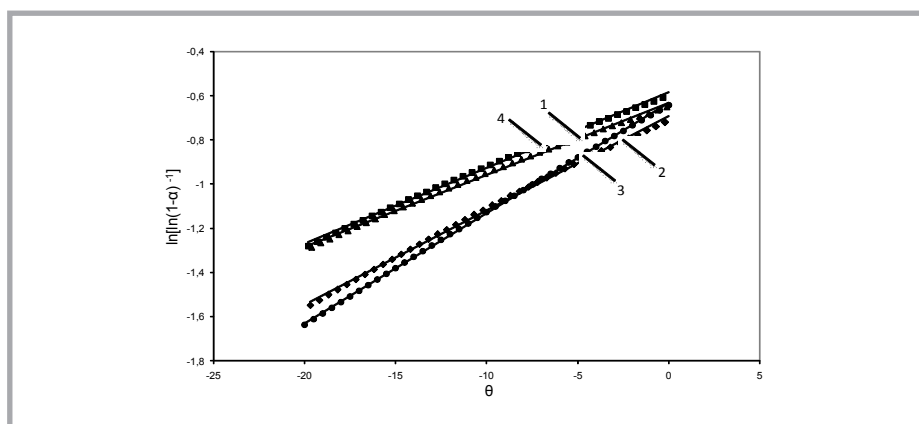


Figure 6. Plot of $\ln[\ln(1-\alpha)^{-1}]$ versus θ (Equation (8)). Weight fraction of a nanofiller equal to 10%. 1 – CH; 2 – CHH; 3 – CHN; 4 – CHAg.

the polymer; the second thermal step occurring in the range 160 – 200 °C is attributed to further dehydration, to acetylation and depolymerization of chitosan. The third step, for temperature higher than 200 °C, corresponds to the residual decomposition reactions. The scope of this work will be focused on the third stage of the thermal degradation in the range 200 – 400 °C. It may be observed that the curves are shifted to higher temperatures as the heating rate increases from 5 C/min to 15.0 C/min (**Figure 4.a**), this effect being more easily observed in the DTG curves. Based on the analysis of thermogravimetric curves some characteristic parameters of blend thermodegradation were determined for the third step of degradation:

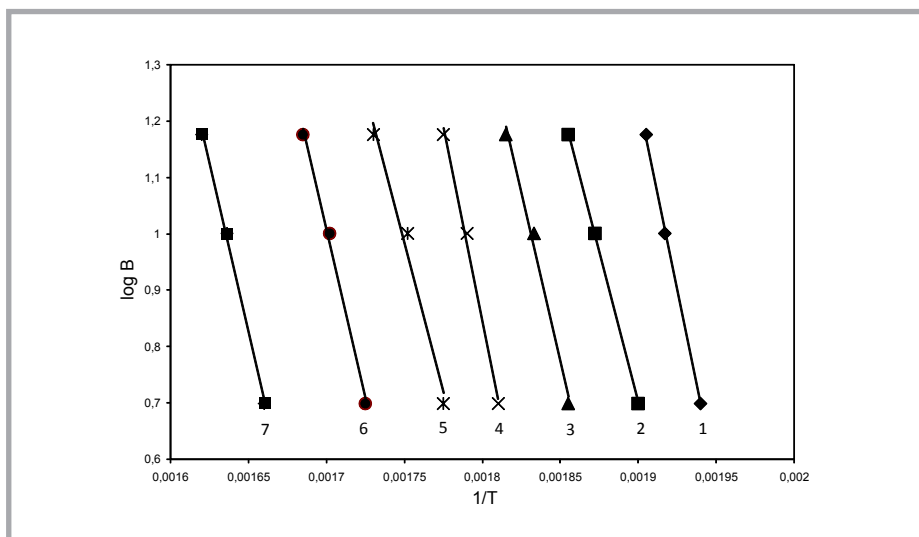


Figure 7. Plot of $\log \beta$ versus $1/T$ (Equation (7)). Figure is drawn for chitosan with nanosilver 10% w/w. 1 denotes α equal to 0.2; 2 – 0.3; 3 – 0.4; 4 – 0.5; 5 – 0.6; 6 – 0.7; 7 – 0.8.

- $T_{5\%}$: temperature of the degradation onset was determined on the basis of the deviation of curve TG from the initial run for zero to 5% value of the conversion degree α ;
- T_{\max} : temperature of the maximum of degradation rate (from DTG).
- E_a – activation energy of main step of decomposition.

The activation energy was calculated using methods by Freeman – Carroll (**Figure 5**) and Horowitz – Metzger (**Figure 6**). The results are summarized in **Table 1**.

To apply the isoconversional method proposed by Ozawa [8] to the first stage of the thermal degradation of chitosan scanned at different heating rates, the extensions of conversion $\alpha = 0$ and $\alpha = 1$ were taken at 200 °C and 400 °C, respectively. Thus the curves $\log \beta$ versus $1/T$ were plotted for experimental data in the range $0.1 < \alpha < 0.8$ (**Figure 7**) allowing the determination of the kinetic parameters E_a (**Table 1**).

4.2. Isothermal experiments – Freedman method [10]

In the isothermal experiments, the chitosan was heated to a temperature approaching the beginning of the first stage of its thermal degradation and it was maintained at this temperature for a given time while the loss of weight was monitored, allowing the calculation of the extension of conversion as a function of the reaction time. To allow an easier comparison of the results of the isothermal experiments with those issued from the dynamic ones, the extension of conversion of the former were normalized with respect to the maximum extension of conversion attained in the dynamic experiments. The experimental data were treated according to the isothermal method. The curves showing the plots of $\ln(d\alpha/dT)$ versus $\ln(1-\alpha)$ as a function of conversion are shown in **Figure 8**, while the values of E_a and n are summarized in **Table 1**.

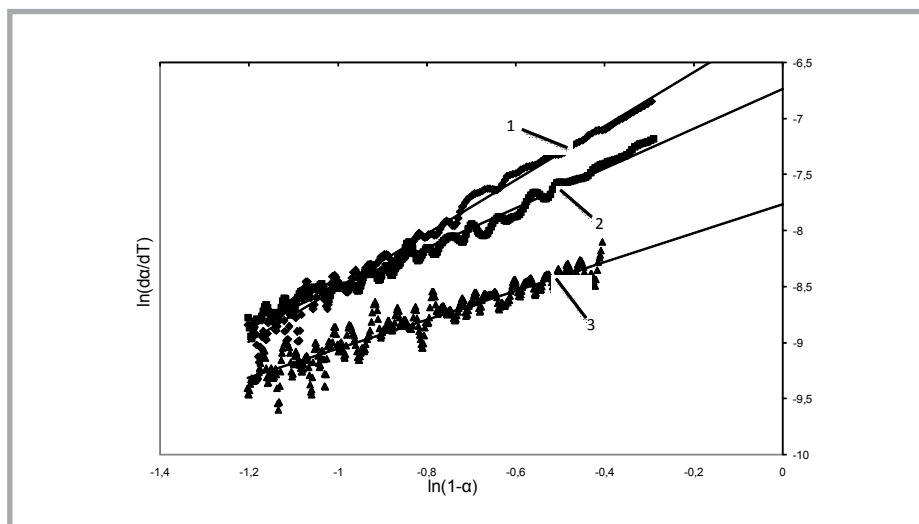


Figure 8. Plot of $\ln(da/dT)$ versus $\ln(1-\alpha)$ (Equation 9). Figure is drawn for chitosan with nanosilver 2%. 1 – denotes temperature 240 °C; 2 – temperature 230 °C; 3 – temperature 220 °C.

Table 1. Degradation parameters for chitosan and its composites.

No.	Sample	E_a , kJ/mol				n	$T_{5\%}$, C	T_{max} , C
		Horowitz-Metzger	Freeman-Carroll	Ozawa	Isothermal method			
1	CH	82.0	75.2	165.5	140.2	2	220	277
2	CHH	104.0	124.7	-	-		172	274
3	CHN	129.5	124.6	-	-		200	279
4	CHAg	103.0	136.6	232.5	-		210	272
5	CHAg2	82.4	94.5	190.9	173.6		220	266

According to the results of this work, the activation energy increases for chitosan with nanofillers when compared to the pure chitosan. It can be noted that in case of chitosan with nanosilver that the activation energy is greater for chitosan with 10% nanosilver (CHAg) than for chitosan with 2% nanosilver.

5. Conclusions

It can be presumed that the observed small improvement of thermal stability of the composites (the increase of activation energies and T_{max}) is attributed to the shielding effect of the clay and hydroxyapatite which means that degradation products can have a long way around the nonorganic compound additives to leave the samples.

Some increase of thermal stability was also observed in literature in a case of thermoplastic starch with unmodified MNT [14]. However, it is difficult to draw a conclusion on the mechanisms of degradation of nanocomposites on the basis of present literature

[15]. The influence of nanofillers on a small weight loss of the samples in the range to 200 °C (7 – 10% for chitosan) requires further discussion.

Two opposing activities of the additives may be predicted in polymeric nano- or microcomposites influencing the thermal stability of material - one was increasing barrier properties and insulating properties to heat transport that should improve the thermal stability and the other is the catalytic effect towards the degradation of the polymer matrix which would decrease the thermal stability. That should depend on intrinsic properties of polymer matrix, on the routes of polymer degradation, amount and dispersion of nanofillers [16]. Furthermore, the authors intend to carry out the FTIR investigations and thermogravimetry in the air atmosphere in the future for comparison.

6. References

1. Muzzarelli R.A.A. (2009); *Chitins and chitosans for the repair of wounded skin, nerve, cartilage and bone*, *Carbohydrate Polymers* Vol. 76, pp. 167-182.
2. Mucha M.; *Chitosan, Versatile Polymer from Renewable Sources*, WNT Warsaw, 2010.
3. Pawlak A., Mucha M.; (2003) *Thermogravimetric and FTIR studies of chitosan blends*, *Termochim. Acta.*, Vol. 396, pp. 153-166.
4. de Brittoa D., Campana-Filho S.P.; (2007) *Kinetics of the thermal degradation of chitosan*, *Termochim. Acta*. Vol. 465, pp. 73-82.
5. Dowling D. P., Donnelly K., McConnell M. L., Eloy R., Arnaud M. N.; (2001) *Deposition of anti-bacterial silver coatings on polymeric substrates*, *T. Sol. Films*, Vol. 398, pp. 602-606.
6. Vyazovkin S., Wight C. A.; (1998) *Isothermal and nonisothermal kinetics of thermally stimulated reactions of solids*, *Int. Rev. Phys. Chem.* Vol. 17, pp. 407-433.
7. Freeman E.S., Carroll B.; (1958) *Interpretation of the kinetics of thermogravimetric analysis*, *J. Phys. Chem.* Vol. 73, pp. 751-752.
8. Ozawa T.; (1970) *Kinetic Analysis of Derivative Curves in Thermal Analysis*, *J. Therm. Anal.* Vol. 2, pp. 301-324.
9. Horowitz H., Metzger G.; (1963) *A new analysis of thermogravimetric traces*, *Anal. Chem.* Vol. 88, pp. 1464 -1468.
10. Friedman J.; (1964) *Kinetics and Mechanism of Vinyl Chloride Polymerization: Effects of Additives on Polymerization Rate, Molecular Weight and Defect Concentration in the Polymer*, *J. Polym. Sci. Polymer Symp.* Vol. 6, pp. 183-195.
11. Mucha M., Matusiak B.; (2009) *Water Sorption Isotherms of Chitosan and Its Blends with Nanofiller*, 9th *International Conference of the European Chitin Society*, *Conference Book*. pp. 140-146.
12. Zanetti M., Camilo G., Mulhaupt R.; (2001) *Combustion behaviour of EVA/fluorohectorite nanocomposites*, *Polymer. Degr. Stab.* Vol. 74, pp. pp. 413-417.
13. Chen G-X., Yoon J-S.; (2005) *Thermal stability of poly(L-lactide)/poly(butylene succinate)/ clay nanocomposites*, *Polymer. Degr. Stab.* Vol. 88, pp. 206-212.
14. Park H.M., Lee W. K., Park C. Y., Cho W. J. & Ha C. S.; (2003) *Environmentally friendly polymer hybrids*. *J. Mat. Sci.* Vol. 38, pp. 909-914.
15. Kumar A. P., Depan D., Tomer N. S., Singh R. P.; (2009) *Nanoscale particles for polymer degradation and stabilization – Trends and future perspectives*. *Progress in Polymer Sci.* Vol. 34, pp. 379-515.
16. Leszczyńska J., Njuguna K., Pielichowski J. R.; (2007) *Polymer/montmorillonite nanocomposites with improved thermal properties. Part II. Thermal stability of montmorillonite nanocomposites based on different polymeric matrixes*. *Termochim. Acta*, Vol. 454, pp. 1-22.

